

# Evaluation of Clean Fractionation Pretreatment for the Production of Renewable Fuels and Chemicals from Corn Stover

Rui Katahira,<sup>†,‡</sup> Ashutosh Mittal,<sup>§</sup> Kellene McKinney,<sup>†,‡</sup> Peter N. Ciesielski,<sup>§</sup> Bryon S. Donohoe,<sup>§</sup> Stuart K. Black,<sup>†</sup> David K. Johnson,<sup>§</sup> Mary J. Bidy,<sup>†,‡</sup> and Gregg T. Beckham<sup>\*,†,‡</sup>

<sup>†</sup>National Bioenergy Center, National Renewable Energy Laboratory, Golden, Colorado 80401, United States

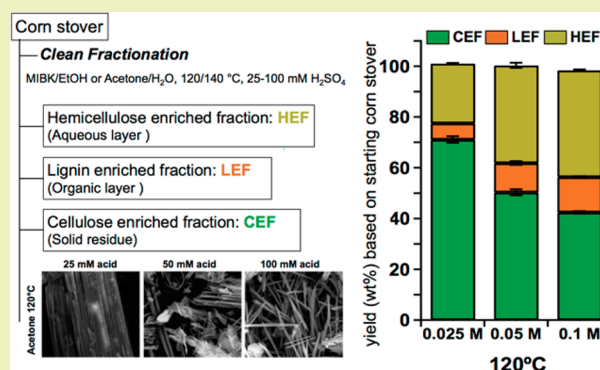
<sup>‡</sup>National Advanced Biofuels Consortium, National Renewable Energy Laboratory, Golden, Colorado 80401, United States

<sup>§</sup>Biosciences Center, National Renewable Energy Laboratory, Golden, Colorado 80401, United States

## S Supporting Information

**ABSTRACT:** Organosolv fractionation processes aim to separate the primary biopolymers in lignocellulosic biomass to enable more selective deconstruction and upgrading approaches for the isolated components. Clean fractionation (CF) is a particularly effective organosolv process that was originally applied to woody feedstocks. The original CF pretreatment employed methyl isobutyl ketone (MIBK), ethanol, and water with sulfuric acid as a catalyst at temperatures ranging from 120 to 160 °C. Understanding the feasibility and applicability of organosolv processes for industrial use requires mass balances on the primary polymers in biomass, detailed understanding of the physical and chemical characteristics of the fractionated components, and viable upgrading processes for each fraction. Here, we apply two CF approaches to corn stover, one with MIBK/ethanol/water and acid and the other with MIBK/acetone/water and acid, with the aim of understanding if these fractionation methods are feasible for industrial application. We quantify the full mass balances on the resulting solid, organic, and aqueous fractions and apply multiple analytical methods to characterize the three fractions. Total mass yields of the cellulose-enriched, hemicellulose-enriched, and lignin-enriched fractions are near mass closure in most cases. For corn stover, the MIBK/acetone/water CF solvent system is more effective relative to the original CF method based on the enhanced fractionation susceptibility of the aqueous and organic phases and the lower molecular weight distribution of the lignin-enriched fractions. Overall, this work reports component mass balances for the fractionation of corn stover, providing key inputs for detailed evaluation of CF processes based on bench-scale data.

**KEYWORDS:** Organosolv, Cellulose, Hemicellulose, Lignin, Biofuels



## INTRODUCTION

Significant research and development efforts have been applied to biomass pretreatment processes for the production of renewable fuels and chemicals from lignocellulose,<sup>1–8</sup> as these unit operations are often the most costly portion of biochemical conversion processes.<sup>6–10</sup> Biomass pretreatment is generally intended to improve the accessibility for enzymes and microbial catalysts to digest the residual solid carbohydrates and in some cases to depolymerize hemicellulose to soluble sugars.<sup>2,7</sup> Many pretreatment processes have been developed, and significant research has been conducted to compare pretreatment processes, for example, in the Consortium for Applied Fundamentals and Innovation (CAFI).<sup>3,5,6</sup> Most pretreatment processes studied in CAFI, which included hot water treatment, dilute acid pretreatment, steam explosion, lime pretreatment, ammonia fiber expansion, and ammonia recycle pretreatment, were focused primarily on the cost-effective depolymerization of sugars for ethanol production. Indeed, biorefineries are now

coming online worldwide that employ several of these technologies.

Going forward, lignocellulosic biorefineries intended to produce fuels and chemicals will undoubtedly need to more completely utilize all the components found in biomass, including lignin.<sup>8</sup> A viable upgrading process for lignin to value-added molecules will likely stimulate the re-evaluation of currently employed biomass conversion strategies to consider the most appropriate means to depolymerize and upgrade both lignin and carbohydrates and fractionate these streams in the most cost-effective sustainable manner for maximum yields. In anticipation of this evolution of the biorefining industry, many process options for biomass fractionation and lignin depolymerization are under intense development. For fractionation, the primary options under investigation to date include the broad

**Received:** February 22, 2014

**Revised:** April 20, 2014

**Published:** May 6, 2014

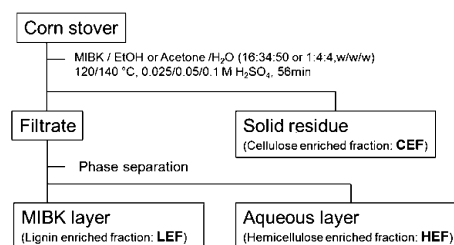
range of processes termed “organosolv” fractionation, wherein organic solvent(s) and water are applied with a co-catalyst, which is typically acidic,<sup>11–14</sup> and more recently developed processes such as ionic liquid fractionation.<sup>15–20</sup>

Organosolv processes have a long history of development. One method developed at the National Renewable Energy Laboratory (NREL), termed clean fractionation (CF), has received significant recent attention for the fractionation of woody feedstocks and grasses.<sup>11,21</sup> This process employs methyl isobutyl ketone (MIBK), ethanol, and water as a solvent system with loadings of sulfuric acid ranging from 0.025 to 0.1 M. CF produces an aqueous–organic phase and a solid cellulose-enriched fraction (CEF). Further manipulation of the liquid phase results in a lignin-enriched fraction (LEF) in the organic phase and an aqueous phase containing monomeric and oligomeric species resulting from hemicellulose hydrolysis in the aqueous hemicellulose-enriched fraction (HEF). This process has also been extended to several lignocellulosic feedstocks including switchgrass, wherein it was shown to be viable for fractionation at the bench scale.<sup>12</sup> For herbaceous feedstocks, however, the original CF experiments utilized sodium chloride to expedite phase separation in laboratory settings for improved partition of the organic and aqueous layers after fractionation. The reason for this is unclear, but presumably it is related to the differences in lignin composition between woody and herbaceous feedstocks.

To understand the potential utility of a given process option, it is essential to build robust techno-economic models based on laboratory or pilot-scale data.<sup>8–10</sup> As yield typically drives the economics of biomass conversion processes,<sup>8–10</sup> it is especially important to conduct quantitative mass balances for various process options. To that end, here we conduct CF of corn stover with the standard MIBK/ethanol/water CF methodology (which we hereafter refer to as “EtOH-CF”) and use an additional CF approach with MIBK/acetone/water (“Acetone-CF”) substituting ethanol with acetone. The advantages of using acetone in the alternative solvent system proposed here are as follows: (1) Acetone exhibits a lower boiling point (56 °C) than ethanol (78 °C), thus simplifying its recovery by distillation. (2) Acetone does not form an azeotrope with water thus making separation of the ketone from the aqueous fraction simpler. (3) An improved phase separation of organic and aqueous fractions was achieved without requiring any addition of sodium chloride for corn stover. (4) The proportions for the mixture in Acetone-CF are adjusted such that the solvent system remains single phase allowing reduction of the MIBK proportion relative to EtOH-CF. As a result, MIBK needed for the process has been substantially reduced. The techno-economic ramifications of this substitution will be examined in a future study from our group.

In the present work, a comparative evaluation of CF of corn stover using two solvent systems (EtOH-CF and Acetone-CF) is conducted. Each CF method is applied at six conditions spanning sulfuric acid loadings from 0.025, 0.05, and 0.1 M at temperatures of 120 and 140 °C, following conditions employed in previous work from Bozell et al.<sup>11,12</sup> and as illustrated in Scheme 1. We examine the mass closure for the three resulting fractions from corn stover for each of the three primary components, lignin, hemicellulose, and cellulose, and then characterize the physical and chemical properties of each fraction with various techniques. This work forms a key resource to build a techno-economic model for CF and demonstrates that using an Acetone-CF method for corn stover

Scheme 1. Schematic of the Clean Fractionation Procedure



results in enhanced fractionation without the need for additional components (e.g., sodium chloride). This work is accompanied by a companion study wherein enzymatic hydrolysis is conducted with multiple types of enzymatic cocktails for cellulose depolymerization with the intent to understand the difference between the effectiveness of CF relative to dilute-acid pretreatment in enabling greater access for cellulase to depolymerize cellulose.<sup>36</sup>

## RESULTS AND DISCUSSION

**Mass Balance.** CF experiments with corn stover (10 g, moisture content 9.735 wt %) were conducted at 120 and 140 °C with sulfuric acid (0.025, 0.05, and 0.1 M) in two different solvent systems: single-phase mixtures of methyl isobutyl ketone (MIBK)/acetone/water (11/44/44, g/g/g, 100 mL) “Acetone-CF” or MIBK/ethanol (EtOH)/H<sub>2</sub>O (16/34/50, g/g/g, 100 mL) “EtOH-CF”<sup>11,12</sup> (Table 1). To evaluate the

Table 1. Clean Fractionation Conditions and Severity Factor

solvent	temp. (°C)	acid concentration (mol/L)	pH	combined severity factor <sup>a</sup> log R <sub>0</sub> – pH
MIBK/acetone/H <sub>2</sub> O	120	0.025	2.17	0.03
	120	0.05	2.02	0.17
	120	0.1	1.72	0.47
	140	0.025	2.71	0.07
	140	0.05	2.16	0.62
	140	0.1	1.99	0.79
MIBK/EtOH/H <sub>2</sub> O	120	0.025	2.12	0.07
	120	0.05	1.94	0.25
	120	0.1	1.62	0.57
	140	0.025	1.93	0.85
	140	0.05	1.82	0.96
	140	0.1	1.52	1.26

<sup>a</sup>Severity factor was calculated for the fractionation time *t* under isothermal conditions, which was 40 min for all the experiments conducted in this study.

separation efficiency for the fractionation conditions employed in this work, the combined severity factor approach<sup>22</sup> is used as it enables the combination of the effect of time, temperature, and catalyst concentration into a single factor R<sub>0</sub>'. The combined severity factor values reported in Table 1 are calculated using the following equation<sup>22</sup>

$$R_0' = \log R_0 - \text{pH}$$

where R<sub>0</sub> is defined as<sup>23</sup>

$$R_0 = t \exp \left[ \frac{T - T_r}{14.75} \right]$$

where  $t$  is the fractionation time under isothermal conditions (40 min),  $T$  is the absolute fractionation temperature, and  $T_r$  is the reference temperature (100 °C).

The composition of the original corn stover is shown in Table 2. After both CF pretreatments, corn stover is

**Table 2. Compositional Analysis in Whole Corn Stover**

component	wt %
lignin	15.0
glucan	37.2
xylan	22.9
galactan	1.4
arabinan	2.9
acetyl	2.9
ash	3.5
protein	2.0
sucrose	4.3
water extractives	7.6
ethanol extractives	2.8
total	95.6

fractionated into aqueous and organic MIBK-rich streams and a residual solid. NaCl was employed previously with switchgrass to enhance separation of the aqueous and organic fractions for the EtOH-CF process.<sup>12</sup> It was noted that NaCl addition was primarily conducted to expedite fractionation but that water alone was sufficient.<sup>12</sup> For EtOH-CF with corn stover, however, addition of 25% v/v deionized water to the aqueous and MIBK stream did not enable phase separation and resulted in the formation of an emulsion. This disparity in fractionation ability is likely due to the differences in lignin and other cell wall polymers between corn stover and switchgrass. In the Acetone-CF method, the addition of solid NaCl or deionized water was not necessary for expedient effective separation, and the separation of an aqueous and organic phase was rapid. Overall, the main components in corn stover were fractionated in three parts: cellulose-enriched fraction (CEF), hemicellulose-enriched fraction (HEF), and lignin-enriched fraction (LEF). For each CF method, we refer to the particular component fraction with the different solvent, e.g., the CEF from the Acetone-CF pretreatment is termed “Acetone-CEF”.

Material balances are essential for determining the fractionation efficiency and also for understanding the appropriateness of the conditions applied in the process, and thus, a mass balance was performed for each CF experiment, as shown in Figure 1. The yield of each of the enriched fractions in the starting corn stover was determined gravimetrically based on dry whole corn stover. Table S1 of the Supporting Information shows the detailed yields of CEF, HEF, and LEF at each CF condition. The total gravimetric yields of all three enriched fractions obtained after CF were 95–104 wt % and 92–103 wt % in Acetone-CF and EtOH-CF cases, respectively, based on the starting corn stover mass. For both CF solvent systems, the fractionation efficiency of the main components in corn stover increases with an increase in the severity of the extractions (Figure 1). For example, in Acetone-CF (Figure 1A) with increasing acid loading from 0.025 to 0.1 M acid at 120 °C, the yield of CEF decreases from 71.1 to 42.4 wt % due to selective fractionation of the hemicellulose and lignin components from the starting corn stover in HEF and LEF, respectively. Consequently, the yield of LEF increases from 6.4 to 14.0 wt % and HEF increases from 23.6 to 42.0 wt %. A

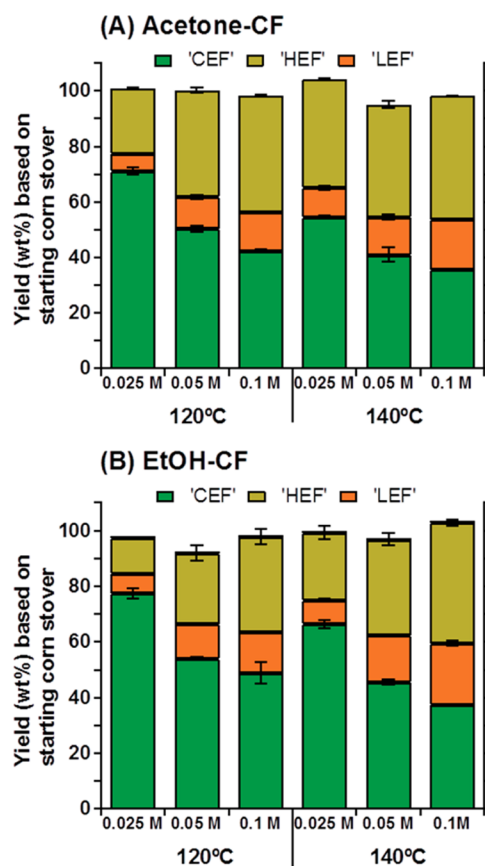


**Figure 1.** Mass yields (wt %) of the three fractions, CEF, HEF, and LEF, following CF. (A) Acetone-CF and (B) EtOH-CF.

higher fractionation efficiency was obtained for each component with increasing acid loading from 0.025 to 0.1 M acid at 140 °C. The yield of the Acetone-CEF decreases from 54.5 to 35.6 wt %, whereas the yield of Acetone-LEF increases from 10.7 to 18.0 wt % and Acetone-HEF increases from 39.0 to 44.7 wt %. The same trend of increasing mass yields of each fraction with an increase in the severity of the extractions was obtained for EtOH-CF (Figure 1B). Comparing the two CF technologies, higher wt % yield for the HEF was obtained in Acetone-CF, whereas higher wt % yields for the CEF and LEF were obtained in EtOH-CF. The overall trends for both CF technologies are reasonably similar in terms of mass yields of each fraction between Acetone-CF and EtOH-CF with the highest fractionation efficiency being achieved at 140 °C and 0.1 M acid in both cases.

The cellulose mass balance closure (MBC) was calculated based on the glucan content in the original corn stover using eq 1. For all components, the recovered amount is across all three streams from CF. For example, “Total cellulose recovered” is the total glucan detected in the CEF, HEF, and LEF. Hemicellulose and lignin MBCs were also calculated similarly.

$$\text{Cellulose MBC (\%)} = \frac{\text{Total glucan recovered (g)}}{\text{Glucan in original corn stover (g)}} \times 100 \quad (1)$$

Figure 2 shows the total MBC for the individual components, cellulose, hemicellulose, and lignin, in the different biomass fractions obtained from the EtOH and Acetone-CF experiments. Table S2 of the Supporting Information shows the detail

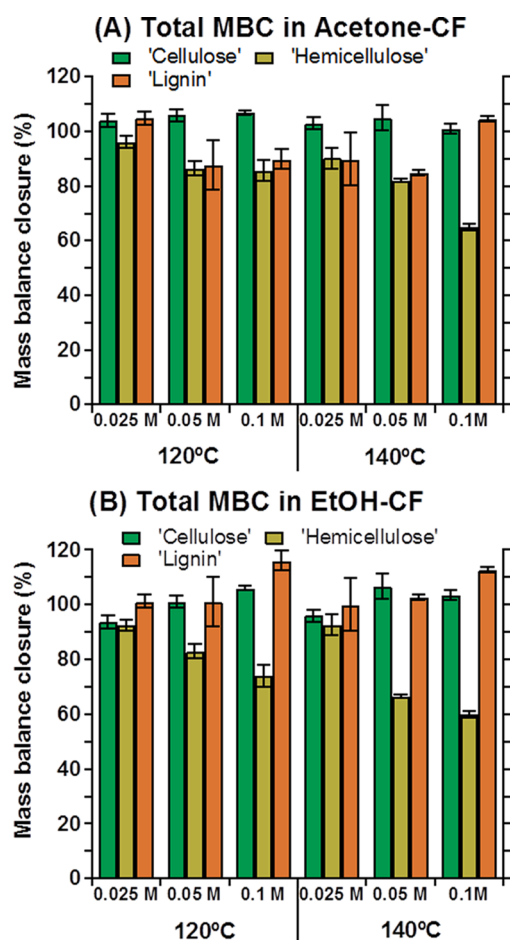


**Figure 2.** Total mass balance closure for cellulose, hemicellulose, and lignin in (A) Acetone-CF and (B) EtOH-CF experiments.

total MBC values under each CF condition. The glucan recovery varies from 101 to 107% in Acetone-CF (Figure 2A) and 94–107% in EtOH-CF (Figure 2B), which suggests that little to no degradation of cellulose was observed in Acetone-CF and that a minor amount of cellulose was degraded in EtOH-CF.

Generally, the recovery of total hemicelluloses decreased in both CF approaches with an increase in the severity of the extractions (Figure 2) where the term “severity” is defined above.<sup>23</sup> The total hemicellulose recovered in the extractions performed at the highest severity with 0.1 M acid at 140 °C are 65% and 60% for Acetone-CF and EtOH-CF, respectively. It is known that in high temperature acidic conditions, xylose undergoes dehydration to yield furfural, which further reacts with itself, xylose, or lignins to yield heterogeneous degradation products.<sup>24</sup> Thus, it is assumed that the low recovery of hemicellulose at higher severity is primarily due to the loss of xylose and arabinose to sugar degradation compounds such as furfural, which was detected in the aqueous fraction in concentrations up to 4.6% on a mass basis of initial xylan. The total lignin recovery obtained increased steadily with increasing severity and reached ~113% in EtOH-CF performed at the highest severity (Figure 2B). This increase in lignin quantity has been reported in earlier literature<sup>25,26</sup> and has been attributed to pseudolignin,<sup>23</sup> comprising carbohydrate degradation products formed during the hydrothermal treatment of lignocellulosic material. Incorporation of ethanol in the LEF is another possibility for the increase, but it could occur to a very

small extent.<sup>27</sup> Comparing both CF approaches, total cellulose MBCs in Acetone-CF are similar to those in EtOH-CF, and hemicellulose and lignin MBCs in Acetone-CF are larger and smaller than those in EtOH-CF, respectively.

To ascertain the fate of each biopolymer during CF, individual mass balances were performed on the glucan, hemicellulose, and lignin present in each fraction, CEF, HEF, and LEF, as shown in Figure 3. Each individual MBC was calculated based on the content of the individual component in the original corn stover using eq 2. The individual MBCs for hemicellulose and lignin were also calculated similarly. For instance, in Acetone-CF at 120 °C with 0.025 M acid, 95% of the total glucan present in the starting corn stover was recovered in CEF, 9.4% in HEF, and 0.2% in LEF (Figure 3A).

Glucan MBC in CEF (%)

$$= \frac{\text{Glucan in CEF (g)}}{\text{Glucan in original corn stover (g)}} \times 100 \quad (2)$$

Tables S3 and S4 of the Supporting Information show the detailed individual mass balances for each CF condition in Acetone-CF and EtOH-CF, respectively. For the glucan mass balance in Acetone-CF (Figure 3A), we observe >90% of the total glucan recovery in the CEF with no influence of acid concentration at 120 °C. However, at 140 °C, the glucan recovery in the CEF decreases with increasing acid loading from 91% to 84% for extractions conducted at 0.025–0.1 M acid. For the glucan mass balance in EtOH-CF, the glucan recovery in the CEF varied between 88.0% and 96.8% showing no influence of temperature or acid concentration (Figure 3B). The recovery of the glucan in the HEF (as glucose) increases slightly with increasing severity and reaches 11–16% in both Acetone-CF and EtOH-CF, whereas no glucan was detected in the LEF (Figure 3A,D). Tables S6 and S7 of the Supporting Information show the detailed compositional analysis for each CF condition in Acetone-CF and EtOH-CF. For both CF methods, the glucan content in CEF increases steadily with increasing temperature and acid concentration approaching a maximum value of 88% and 82% for Acetone-CF and EtOH-CF, respectively, at 140 °C and 0.1 M acid. The residual hemicellulose and lignin contents in CEF obtained at 140 °C and 0.1 M acid are <5% each for EtOH-CF and <3% each for Acetone-CF. The composition of the CEF obtained in this work with corn stover is similar to that reported for hardwoods<sup>11</sup> using the MIBK/EtOH solvent system under similar fractionation conditions.

Both temperature and acid have a strong influence on hemicellulose recovery. Carbohydrate analysis of the aqueous fractions show that at the lowest severity for both CF approaches, about 92–95% of hemicellulose is recovered with about 67–69% in the CEF and 25–27% in the HEF in Acetone-CF and EtOH-CF, whereas at highest severity, about 60–65% of hemicellulose is recovered with about 2.9–4.3% in the CEF and 56–60% in the HEF (Figure 3B,E). The hemicellulose content in the CEF decreased steadily with increasing acid concentration from 69% to 15% at 120 °C and from 40% to 4.3% at 140 °C in Acetone-CF and from 67 to 26% at 120 °C and from 47 to 2.9% at 140 °C in EtOH-CF. Lower hemicellulose contents are detected in CEFs at higher temperature. Contrastively, the hemicellulose content in HEF increased with higher acid concentration and reached 74% and 49% at 120 °C and 60% and 56% at 140 °C with 0.1 M acid in Acetone- and EtOH-HEFs. No significant amount of hemi-

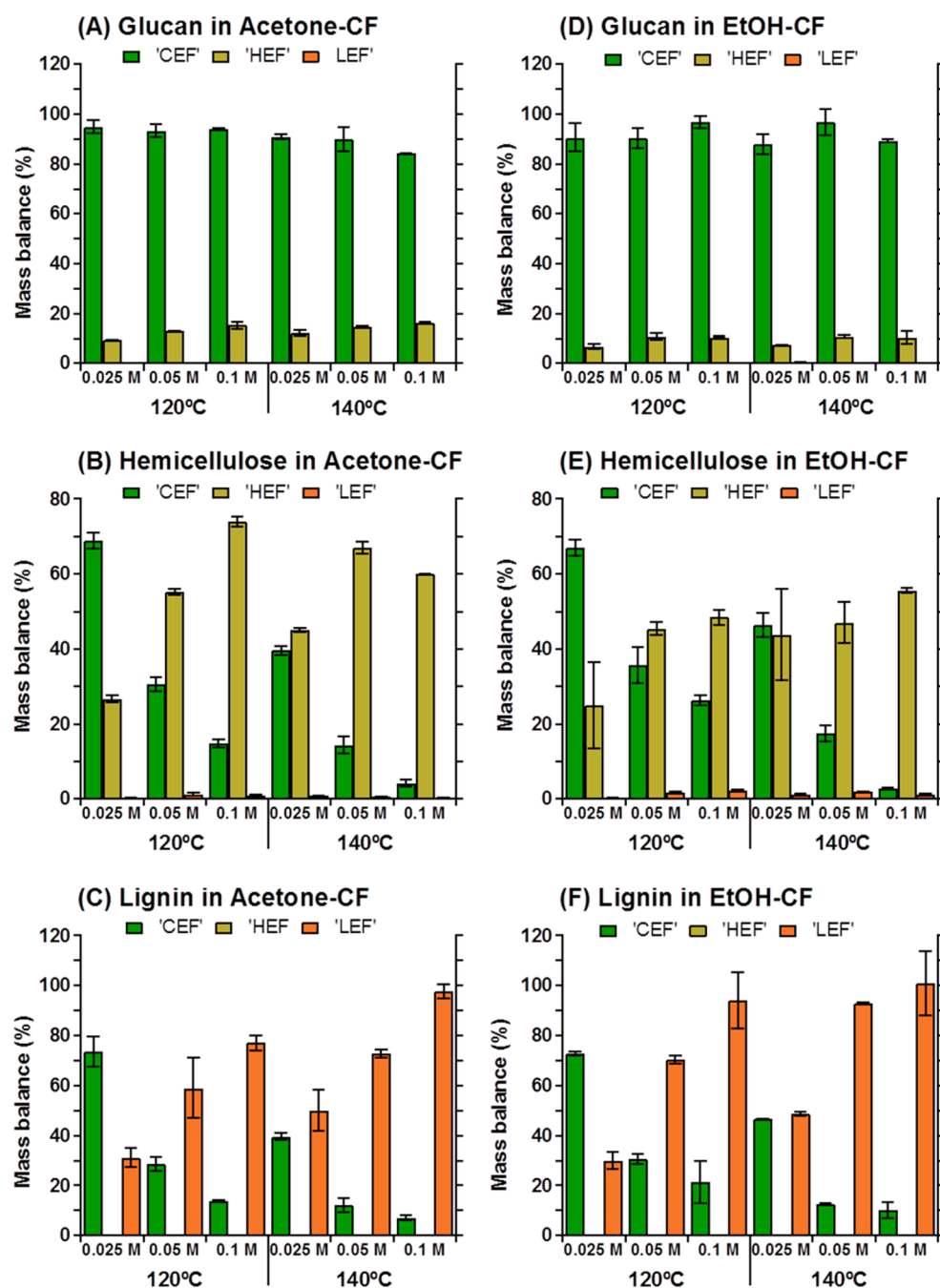


**Figure 3.** Individual mass balances for (A) glucan, (B) hemicellulose, and (C) lignin in Acetone-CF, and (D) cellulose, (E) hemicellulose, and (F) lignin in EtOH-CF. Mass balance of glucan was calculated based on original glucan content. Mass balances of hemicellulose and lignin were calculated similarly.

cellulose was directly detected in the LEF (Tables S6 and S7, Supporting Information). These data indicate that efficiency of hemicellulose fractionation increases with higher acid loading and at higher temperature. However, decomposition of the hemicellulose also makes progress, and efficiency is higher in Acetone-CF.

The recovery of lignin in the LEF increased with increasing severity in both Acetone-CF and EtOH-CF, reaching 97.6 and 100.9%, respectively, whereas it decreased to 7% and 10.2% in the CEF in Acetone-CF and EtOH-CF, respectively (Figure 3C,F). According to the compositional analysis of LEFs (Tables S6 and S7, Supporting Information), the Acetone-LEF and EtOH-LEF at 120 °C with 0.1 M acid gave maximum lignin

contents of 85.5% ( $\pm 5.9\%$ ) and 81.2% ( $\pm 4.8\%$ ), respectively. Lignin contents for the EtOH-LEFs show a positive trend with both temperature and acid concentration; however, no trend for lignin contents was observed for Acetone-LEFs in this work. The LEF samples obtained at fractionation with moderate severity, i.e., 120 °C, 0.1 M acid and 140 °C, 0.025 M acid (Table 1) gave lignin values of 74–79% for both Acetone-CF and EtOH-CF (Tables S6 and S7, Supporting Information). These results are similar to those obtained for corn stover<sup>28</sup> and switchgrass<sup>29</sup> using ethyl acetate as the lignin solvent and for switchgrass<sup>12</sup> using the MIBK/EtOH solvent system. Overall, the individual mass balance results clearly show that CF

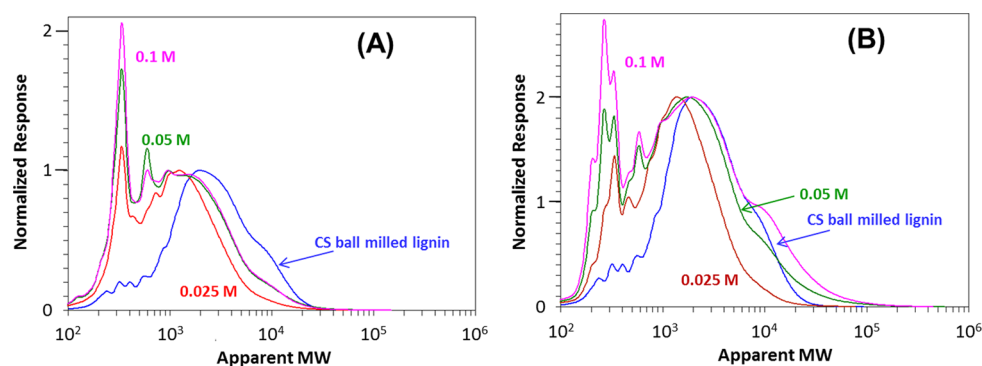


**Figure 4.** Gel permeation chromatograms of lignin-enriched fraction after clean fractionation at 120 °C. (A) Acetone-CF and (B) EtOH-CF compared with  $M_w$  of corn stover ball-milled lignin.

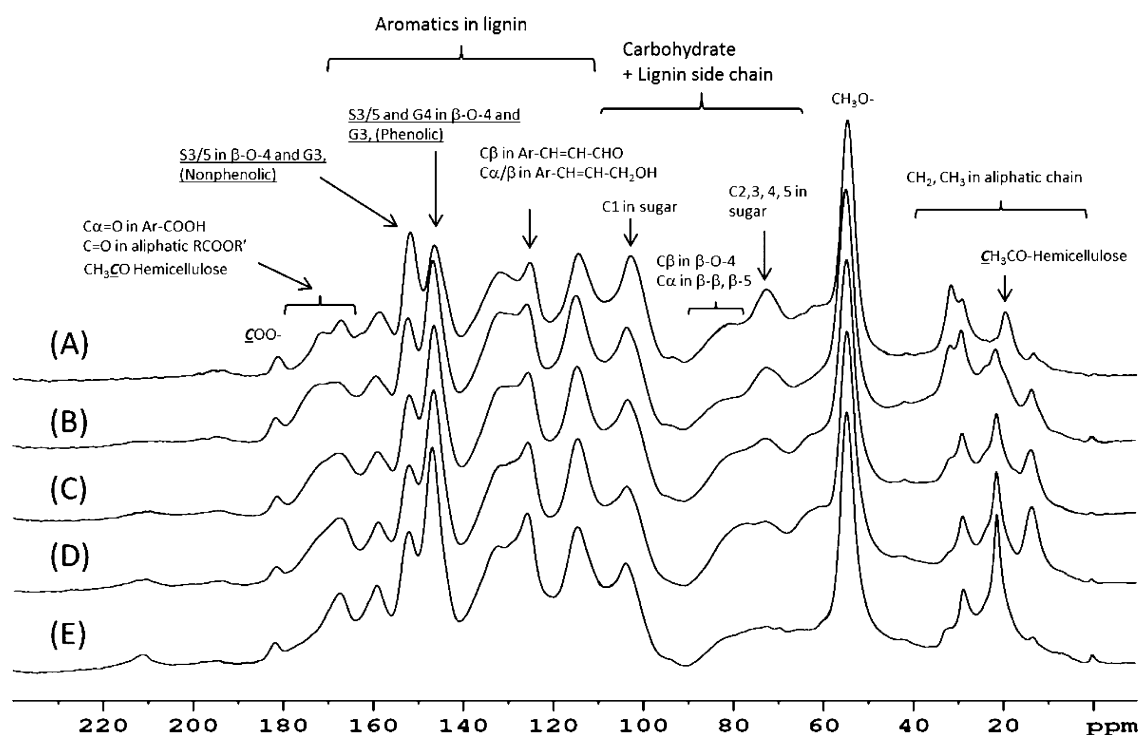


**Figure 5.**  $^{13}\text{C}$  solid-state NMR spectra of corn stover ball-milled lignin and CF lignin-enriched fraction generated at 120 °C in EtOH-CF and Acetone-CF with various acid loadings. (A) Corn stover ball-milled lignin, (B) EtOH-LEF/0.025 M acid, (C) EtOH-LEF/0.05 M acid, (D) EtOH-LEF/0.1 M acid, and (E) Acetone-LEF/0.1 M acid.

effectively fractionates the biomass components to enrich the cellulose and lignin to more than 90% purity.

**GPC Analysis.** The utilization of an organosolv process is partially predicated on the basis of separately and selectively upgrading each fractionated stream. The molecular weight ( $M_w$ ) distribution and the chemical nature of the resulting lignin in the organic phase will dictate the downstream options. Thus, to understand how the CF process affects the  $M_w$  distributions of the lignin streams for subsequent upgrading, CF-LEFs were analyzed by gel permeation chromatography (GPC). GPC chromatograms of LEFs are shown in Figure 4A,B. In both Acetone-LEF and EtOH-LEF, the  $M_w$  distributions in GPC chromatograms have bimodal peaks, which belong to high  $M_w$  components with a large broad peak in the range of 400–10 000 Da and low  $M_w$  species with narrower peaks in the range of 150–400 Da. In Acetone-CF, the LEF obtained with 0.025 M acid has lowest  $M_w$  distributions, and LEFs with 0.05 and 0.1 M acid are similar,

suggesting that a higher acid concentration produces higher  $M_w$  CF-lignin. The weight-average molecular weight of Acetone-LEF at 120 °C with 0.1 M acid was  $M_w = 1600$ , lower than that observed in corn stover lignin ( $M_w = 3700$ ). These results indicate that ether and ester bonds in native corn stover lignin were cleaved during the CF process to give lower  $M_w$  components with weak acid, but both reactions of degradation and repolymerization of the degradation products occurred simultaneously with higher acid concentration. Comparing the Acetone-LEF to the EtOH-LEF at 120 °C, Acetone-LEFs have much lower  $M_w$ . The  $M_w$  of Acetone-LEFs with 0.025, 0.05, and 0.1 M acid were 1600, 2000, and 1900 Da, respectively, whereas those in EtOH-LEFs were 1900, 3700 and 4400 Da, respectively. It was found from this result that efficiencies of degradation and fractionation of CS lignin in Acetone-CF was higher than those in EtOH-CF. The UV spectra during the elution of the higher  $M_w$  components were similar to those of corn stover lignin over the  $M_w$  range from 500 upward to

**Table 3. Structural Characteristics (lignin interunit linkages and S/G ratio) from Integration of  $^{13}\text{C}$ - $^1\text{H}$  Correlation Peaks in the HSQC Spectra of the CF Lignin-Enriched Fraction from Corn Stover<sup>a</sup>**

solvent/material	temp. (°C)	acid concentration (mol/L)	lignin interunit linkages							S/G ratio
			$\beta$ -O-4 (A)	oxidized $\beta$ -O-4 ( $A_{\text{ox}}$ )	Total $\beta$ -O-4 (A + $A_{\text{ox}}$ )	phenyl coumaran (B)	$\beta$ - $\beta$ resinol (C)	dibenzodioxocin (D)	$\beta$ -O-4/methoxy	
CS ball-milled lignin	—	—	78.1%	10.8%	88.8%	2.7%	3.4%	5.1%	0.37	1.25
MIBK/acetone/ $\text{H}_2\text{O}$	120	0.025	73.8%	13.8%	87.6%	3.3%	4.5%	4.7%	0.27	1.36
		0.05	71.9%	16.2%	88.1%	3.9%	4.3%	3.7%	0.15	1.12
		0.1	73.1%	13.4%	86.5%	4.8%	5.8%	2.8%	0.14	1.21
	140	0.025	68.8%	14.0%	82.7%	5.2%	7.4%	4.6%	0.25	1.42
		0.05	70.1%	16.5%	86.6%	4.4%	4.8%	4.2%	0.13	1.10
		0.1	69.0%	17.8%	86.8%	3.8%	4.8%	4.6%	0.07	1.26
MIBK/EtOH/ $\text{H}_2\text{O}$	120	0.025	72.1%	12.0%	84.2%	3.9%	7.3%	4.7%	0.30	1.86
		0.05	71.1%	13.1%	84.2%	4.4%	6.4%	5.0%	0.28	1.45
		0.1	71.0%	11.8%	82.9%	5.8%	7.0%	4.4%	0.10	1.21
	140	0.025	69.4%	14.2%	83.6%	4.8%	7.0%	4.6%	0.23	1.45
		0.05	63.2%	20.3%	83.5%	6.8%	5.2%	4.4%	0.03	0.77
		0.1	68.6%	9.1%	77.7%	8.7%	8.8%	4.8%	0.05	1.01

<sup>a</sup>Each percentage was calculated based on total integration of five main interunits (A,  $\beta$ -O-4;  $A_{\text{ox}}$ , oxidized  $\beta$ -O-4; B, phenylcoumaran; C, resinol; and D, dibenzodioxocin).

10,000, but the UV spectra of the low  $M_w$  species are quite different from those of corn stover lignin, suggesting that nonlignin compounds, i.e., low  $M_w$  sugar degradation products, were generated and fractionated in LEF. GPC chromatograms in Acetone-LEF and EtOH-LEF at 140 °C (data not shown) are similar to those at 120 °C (shown in Figure 4). Overall, two reactions proceed during Acetone-CF and EtOH-CF processes: lignin degradation due to cleavage of ether and/or ester linkages and condensation of low  $M_w$  lignin.

**Solid-State NMR Analysis.** It is important to understand chemical structures in lignin for subsequent utilization, and solid-state nuclear magnetic resonance (NMR) spectroscopy can provide general chemical features of lignin without any derivatization and solubilization.  $^{13}\text{C}$  solid-state NMR spectra of EtOH-LEFs at 120 °C with 0.025, 0.05, and 0.1 M acid and Acetone-LEFs at 120 °C and 0.1 M acid are shown in Figure 5 to evaluate the changes that occur in the chemical structure during CF. Aromatic carbon peaks and unsaturated carbon peaks in side chains appear in the range of 110–165 ppm. Peaks at 146–148 ppm are assigned as aromatic carbons at the 3 and 5 positions in syringyl units (S3/S), 4 position in guaiacyl units (G4) in phenolic  $\beta$ -O-4 units, and 3 position in guaiacyl units (G3) in phenolic units. Peaks at 150–153 ppm are also assigned to be S3/S in nonphenolic  $\beta$ -O-4 units and G3 in nonphenolic units. The ratio of peak area of the phenolic peaks at 146–148 ppm to the peaks at 150–153 ppm increased with increasing acid concentration (Figure 5B–D). This indicates that the LEFs have higher phenolic-OH than original corn stover lignin, meaning some of  $\beta$ -O-4 linkages were cleaved. Peaks of C $\beta$  in cinnamaldehyde units at 126 ppm, C $\alpha$ / $\beta$  in cinnamic alcohol at 128–129 ppm, and C $\alpha$ =O in carboxyl groups at 165–167 ppm increase, and C=O in ester groups in carbohydrates decrease with increasing acid concentration (Figure 5B–D). This suggests that ester linkages between carbohydrate and lignin through cinnamic units are extensively cleaved with higher acid loading. Peaks of C1 at 104–105 ppm and C2,3,5 at 70–76 ppm in cellulose and peaks of C1 at 103–104 ppm and C2,3,4 at 705 ppm in xylan decreased with higher acid loading, which is consistent with higher lignin content in LEFs with increasing acid loadings (Figure 3F). Comparison of

the spectrum of Acetone-LEF with that of EtOH-LEF in the aromatic region (110–165 ppm) reveals that the aromatic structures of both CF-LEFs are similar (Figure 5D,E). Peaks in the region of 56–95 ppm in the EtOH-LEF are larger than those in acetone-LEF. This is because the EtOH-LEFs at 120 °C have slightly higher hemicellulose content (0.5–2.3%) than Acetone-LEF (0.2–1.1%) (Figure 3B,E) and that the EtOH-LEFs have more  $\beta$ - $\beta$  and/or  $\beta$ -5 substructures, which agrees with HSQC-NMR data that EtOH-LEF at 120 °C have 3.9–5.8% of unit B and 6.4–7.3% of unit C, whereas Acetone-LEF have 3.3–4.8% of unit B and 4.3–5.8% of unit C (Table 3).

**Two-Dimensional NMR Analysis (HSQC).** CF-LEFs were analyzed by heteronuclear single quantum coherence (HSQC) NMR spectroscopy, which provides the  $^1\text{H}$ - $^{13}\text{C}$  correlation to obtain chemical structural information related to various lignin interunit linkages and remaining carbohydrates. Figure 6 shows the HSQC NMR spectrum of the Acetone-LEF (140 °C, 0.05 M acid). The spectrum consists of three regions: aromatic

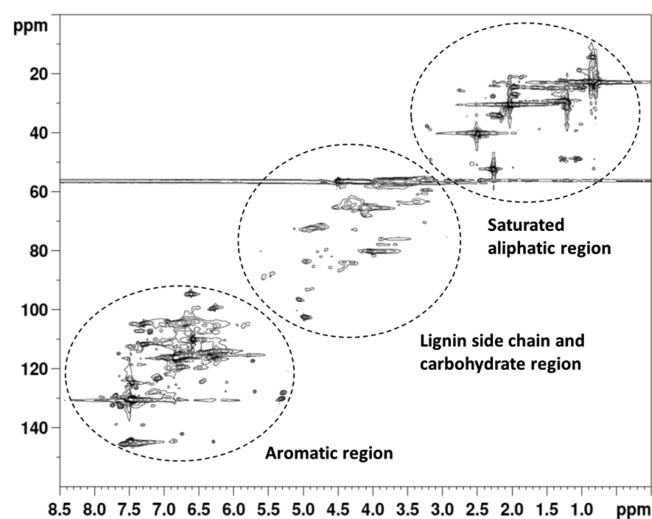


**Figure 6.** HSQC NMR spectrum of lignin-enriched fraction after clean fractionation from corn stover (Acetone-CF, 140 °C, 0.05 M acid, *d*-DMSO).

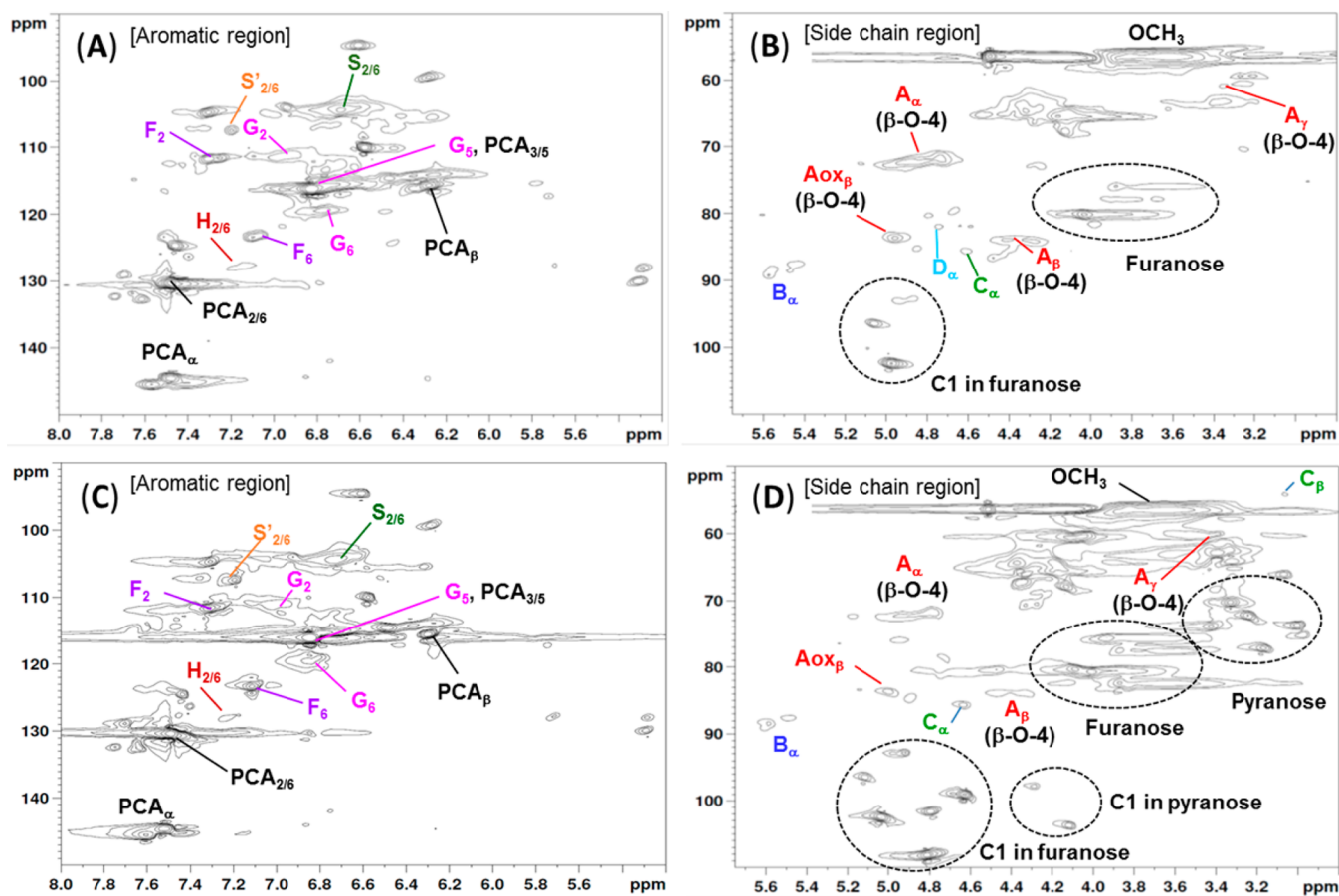


**Figure 7.** Expanded HSQC NMR spectra of CF lignin-enriched fraction from corn stover at 140 °C with 0.05 M acid. (A) and (B) in Acetone-CF and (C) and (D) in EtOH-CF. (A) and (C): Aromatic region ( $\delta_c/\delta_H$  150–100/8.0–5.2 ppm). (B) and (D): Side chain region ( $\delta_c/\delta_H$  110–50/5.7–2.8 ppm).

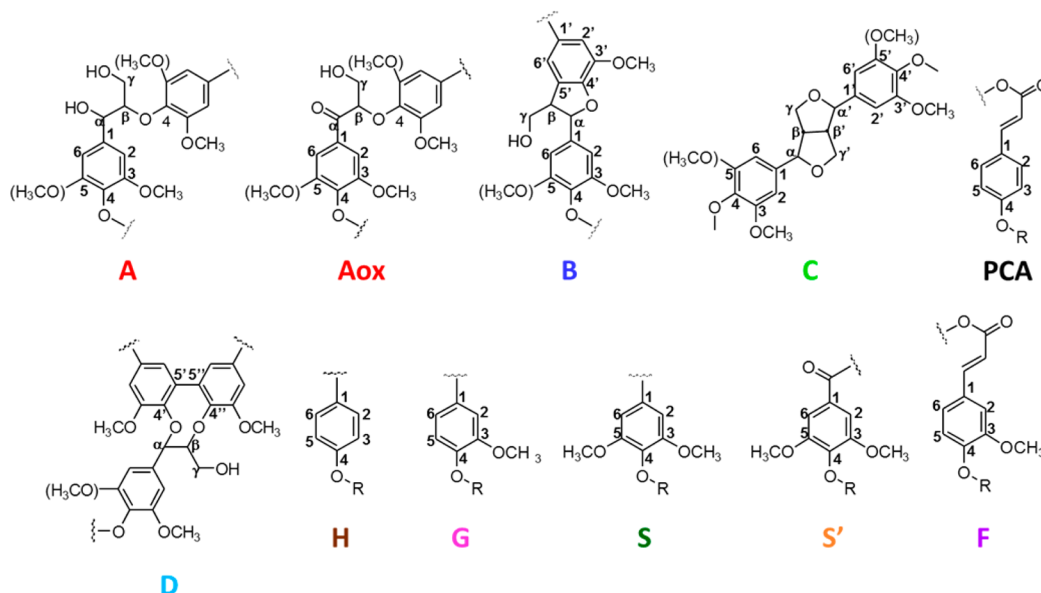


**Figure 8.** Structures of identified lignin units: A,  $\beta$ -O-4 ether linkage; Aox,  $\alpha$ -oxidized  $\beta$ -O-4 ether linkage, B, phenylcoumaran; C, resinol; D, dibenzodioxocine, H, *p*-hydroxyphenyl, G, guaiacyl unit; S, syringyl unit; S', oxidized syringyl unit; F, ferulic acid ester, and PCA, *p*-coumaric acid.

region ( $\delta_c/\delta_H$  95–150/5.3–8.0 ppm), side chain region ( $\delta_c/\delta_H$  55–110/5.7–2.8 ppm), and saturated aliphatic region ( $\delta_c/\delta_H$  10–55/0.5–3.0 ppm).

Figure 7 shows expanded spectra for the aromatic and side chain regions in Acetone-LEF and EtOH-LEF prepared at 140 °C with 0.05 M acid. The typical lignin linkages in biomass are shown in Figure 8. Signals were assigned by HSQC data



previously reported.<sup>12,25,26</sup> In the HSQC spectrum of the aromatic region, aromatic peaks in *p*-hydroxyphenyl (H), guaiacyl (G), syringyl (S) *p*-coumarate (PCA), and ferulate (F) units were observed in both LEFs (Figure 7A,C). Peak areas for S2/6 at  $\delta_c/\delta_H$  104.1/6.7 in the Acetone-LEF are slightly higher than those in the EtOH-LEF, whereas the peak areas for G2 at  $\delta_c/\delta_H$  110.6/6.9 and G6 at 118.2/6.73–6.87 ppm in Acetone-LEF (Figure 7A) are the same as those in the EtOH-LEF (Figure 7C), implying that Acetone-LEF has a higher S/G ratio than EtOH-LEF under the CF conditions at 140 °C with 0.05 M acid. The *p*-coumarate (PCA) peaks of C2/6, C3/5, and C $\alpha$  at  $\delta_c/\delta_H$  131.2/7.5, 115.6/6.8, and 144.7/7.4–7.6 ppm, respectively, are smaller in Acetone-LEF than in EtOH-LEF. Ferulate peaks of F2 at  $\delta_c/\delta_H$  110.2–112/7.21–7.35 and F6 at 122–124/7.03–7.15 ppm in Acetone-LEF exhibit the same trend as PCA. These results suggest that ester linkages between cinnamic acid derivatives in lignin (F and PCA units) and carbohydrates in EtOH-LEF were more abundant than those in Acetone-LEF. The peaks of C2/H2 in the G unit and C2,6/H2,6 in the S unit, which have carbonyl groups at the  $\alpha$ -position, appeared at 122–124/7.4–7.5 and 107/7.2 ppm, respectively.<sup>3b</sup> Comparing those peaks in Figure 7A and C, it was found that the relative amounts of G and S units with C $\alpha$ =O in Acetone-LEF are similar to those in EtOH-LEF at 140 °C with 0.05 M acid. The peaks of C2,6/H2,6 in the H unit with C $\alpha$ =O at 149/8.1 ppm are not found in both LEFs at the CF conditions, but the peaks could appear at higher CF conditions like EtOH-LEF of switchgrass.<sup>3b</sup> In the HSQC spectrum in the side chain region, signals in each unit of  $\beta$ -O-4 (A), C $\alpha$ -oxidized  $\beta$ -O-4 (Aox), phenylcoumaran (B), resinol (C), and dibenzodioxocine (D) appeared (Figure 7B,D). Signals at  $\delta_c/\delta_H$  71–73/4.7–5.0 and 83–84/4.2–4.5 ppm are consistent with the C $\alpha$ /H $\alpha$  and C $\beta$ /H $\beta$  positions in  $\beta$ -O-4 units (A). The peaks in A $\alpha,\beta$  and Aox $\beta$  at 82.7/5.0 ppm in acetone-LEF are larger than those in EtOH-LEF, indicating that acetone-LEF contains more  $\beta$ -O-4 subunits. Signals at  $\delta_c/\delta_H$  88/5.5, and 85/4.65 ppm are also consistent with the C $\alpha$ /H $\alpha$  position in phenylcoumaran (B) and resinol (C) units, respectively. Both peak intensities are low and similar in both LEFs, while the prominent signal of C $\alpha$ /H $\alpha$  in the  $\beta$ -O-4 unit (A) is detected in both LEFs under the CF condition. Peaks of the C $\alpha$ /H $\alpha$  in units B and C gradually increase at 120 °C with increasing acid loadings but decreased at 140 °C with 0.1 M acid in Acetone-LEF, implying that condensation reactions occurred at lower temperature, whereas C–C bonds were also cleaved under more severe CF conditions. The peaks from  $\beta$ -O-4 subunits (A $\alpha,\beta,\gamma$ ) also gradually decreased at increasing fractionation severity. The C $\alpha$ /H $\alpha$  signal in the dibenzodioxocine unit (D) appeared at  $\delta_c/\delta_H$  82/4.75 ppm in only the Acetone-LEF, likely because the  $\beta$ -5 linkage in a phenylcoumaran unit was cleaved and then condensed with a  $\beta$ -O-4 unit to produce a dibenzodioxocine unit (D).

As shown in EtOH-LEF (Figure 7D), anomeric carbon peaks in furanose units appeared at  $\delta_c/\delta_H$  92–110/4.6–5.2 ppm and those in pyranose units at  $\delta_c/\delta_H$  97–104/4.1–4.35 ppm. Larger peak intensity of furanose than that of pyranose means that xylan and arabinan are predominant in the remaining carbohydrates in the EtOH-LEF. This is consistent with compositional analysis data of 3.0% of pentosan and 0.5% of hexosan in EtOH-LEF (Table S7, Supporting Information). On the other hand, only anomeric carbon peaks in furanoses were observed in Acetone-LEF, suggesting that the Acetone-LEF contains less carbohydrate than with EtOH-LEF. This is

supported by the individual mass balance of glucan and hemicellulose (Figure 3A,B,D,E); the individual mass balances of glucan and hemicellulose in Acetone-LEF at 140 °C with 0.05 M acid are 0.25 and 0.69% (Table S3, Supporting Information), respectively, lower than 0.23 and 1.99% in the EtOH-LEF (Table S4, Supporting Information). As the EtOH-LEF has more cinnamic acid derivatives (F and PCA) mentioned above, it could be said that the EtOH-LEF has more lignin–hemicellulose (xylan and arabinan) complexes. Peak intensities of furanose in both LEFs decreased with higher acid condition, meaning that fractionation was facilitated by higher acid loading.

**Semi-Quantification of Interunit Linkages.** Table 3 shows relative percentages of each interunit in the five main interunits (A,  $\beta$ -O-4; A<sub>ox</sub>, oxidized  $\beta$ -O-4; B, phenylcoumaran; C, resinol; and D, dibenzodioxocin) analyzed by HSQC, which do not mean absolute percentages of them in each LEF. The percentage of each linkage was calculated based on the total amount of integration of each cross-peak on the HSQC NMR spectra (Figure 7). The changes in the interunits were independent of the two solvent systems used in this work. The percentages of  $\beta$ -O-4 units (Figure 8A) in all LEFs decreased slightly with an increase in CF temperature to 69–74% in Acetone-LEFs and 63–72% in EtOH-LEFs from 78% in the original corn stover lignin but did not change with increasing acid concentration. The percentages of oxidized  $\beta$ -O-4 structure (A<sub>ox</sub>) did not show any clear trend. Taken together, the percentage of total  $\beta$ -O-4 units in the five main substructures slightly decreased after CF. The phenylcoumaran (B) and resinol (C) units increased a little with increasing acid loading and reaction temperature, whereas dibenzodioxocin units (D) decreased slightly, suggesting that cleavage of ether bonds ( $\alpha$ -O-4,  $\beta$ -O-4, and  $\alpha$ -O- $\gamma$ ) was restricted to C $\beta$ -CS' and C $\beta$ -C $\beta'$  bonds in units B and C, respectively. The peak ratio of  $\beta$ -O-4 ( $\delta_c/\delta_H$  70–74/4.6–5.0 ppm) /methoxyl ( $\delta_c/\delta_H$  55–58/3.4–3.9 ppm) decreased from 0.37 to 0.05 with an increase in the severity of CF conditions, meaning that at least 86% of  $\beta$ -O-4 linkages were probably cleaved with 0.1 M acid at 140 °C in EtOH-CF. This extensive cleavage of  $\beta$ -O-4 linkages was consistent with the increasing trend of peaks of S3/5 and G3/4 in phenolics on the solid-state <sup>13</sup>C NMR (Figure 5).

The S/G ratio with low acid concentration (0.025 M) (1.36–1.86) was higher than original (1.25) and decreased slightly with higher acid loading in LEF. This suggests that more S units are fractionated into LEFs at lower acid loadings resulting in an increase in the S/G ratio, whereas at higher acid loadings, more G units are fractionated resulting in a decrease in the S/G ratio.

**FTIR Analysis.** Fourier transform infrared spectroscopy (FTIR) can provide additional information on the chemical structure of lignin and was applied to the CF lignins. FTIR spectra of the EtOH-LEF and Acetone-LEF produced at 120 or 140 °C with 0.1 M acid are shown in Figure S1 of the Supporting Information. All four FTIR spectra of the LEFs are quite similar. The peak at 1030–1035 cm<sup>-1</sup> is assigned to C–H bonds on the aromatic ring and C=O and C–O stretching in primary alcohol in aromatic constituents rather than sugars because a sample with higher sugar content should have much stronger peaks in the region of 950–1300 cm<sup>-1</sup>, which overlap with the lignin peaks in this region. The EtOH-LEF at 120 °C has the highest absorbance at 1030–1035 cm<sup>-1</sup> and the Acetone-LEF at 140 °C has lowest. This is due to OH peaks from the residual carbohydrates in the EtOH-LEF, which is

supported by compositional analysis data in each LEF. The EtOH-LEF at 120 °C has 4.1% of the total percentage of glucan and hemicellulose, higher than other LEFs (Tables S6 and S7, Supporting Information), and the Acetone-LEF at 140 °C has the lowest percentage of 0.8% (Table S6, Supporting Information). The FTIR peak at around 1200  $\text{cm}^{-1}$  from C–C bonds was higher in LEFs than in the corn stover lignin. This suggests that condensation reactions have occurred with higher acid loading, which is in agreement with the higher  $M_w$  in LEFs with 0.1 M acid shown by GPC analysis (Figure 4). Moreover, peaks at around 1240  $\text{cm}^{-1}$  from ether bonds connected with aromatic rings ( $\beta$ -O-4,  $-\text{OCHH}_3$ ) are lower in the LEFs than that in the corn stover lignin, indicating that some amount of the lignin aryl ether bonds were cleaved. These phenomena are consistent with the cleavage of 86% of  $\beta$ -O-4 linkages measured by HSQC NMR analyses (Table 3).

**Imaging.** The morphology of the CEF is an important factor in determining the effectiveness of a given pretreatment strategy and a means to understanding the enzymatic digestibility of the residual polysaccharides. Table S5 of the Supporting Information shows that the crystallinity of the substrate does not change significantly with CF pretreatment. Scanning electron microscopy (SEM) of the CF cellulose-enriched fractions revealed various degrees of cell separation, which generally increased with increasing treatment severity and extent of lignin extraction. Relatively low acid concentrations (far left column, Figure 9) resulted in more intact clusters of cells and vascular bundles, while increasing acid

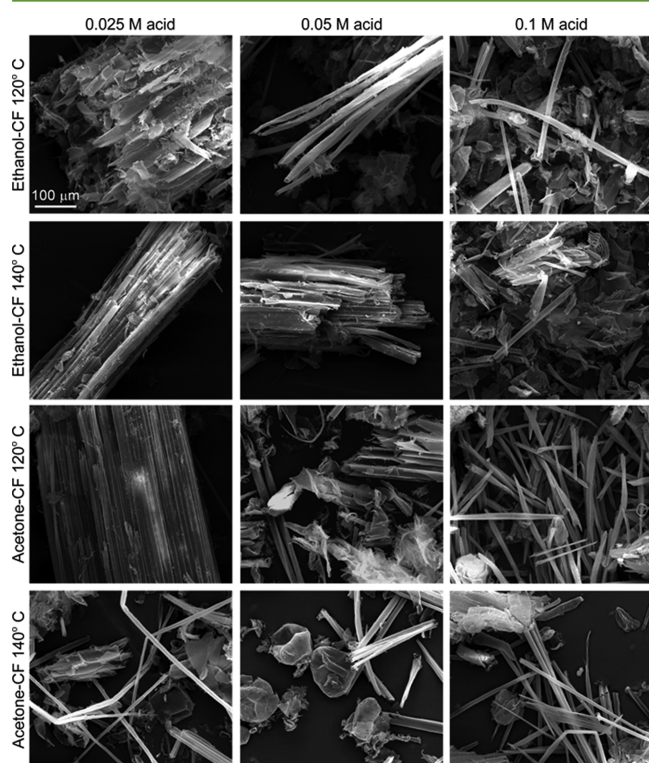


**Figure 9.** Scanning electron microscopy (SEM) of corn stover CEF following CF pretreatment. CF cellulose-enriched fractions display reduced inter cell adhesion that becomes more dramatic at higher treatment severities. Disjoined fiber cells are observed as scattered tubes in samples treated by 0.05 and 0.1 M  $\text{H}_2\text{SO}_4$  in both solvents. The most complete disassembly of cellular bundles was observed in samples treated in acetone at the two higher acid loadings.

concentration and temperature produced biomass with decreased intercell adhesion. Complete disjoining of cells, observed as scattered tubular structures in the case of fiber cells, was present in samples treated at intermediate acid concentrations (middle column, Figure 9). Cell separation was extensive throughout samples treated by 0.1 M acid in EtOH–CF and nearly complete when the same acid concentration was used in Acetone–CF.

This cellular-scale particle morphology is similar to that produced by other pulping and pretreatment processes.<sup>30</sup> This effect primarily results from the removal of the lignin-rich middle lamellar region of the cell walls, which dramatically reduces intercell adhesion of the remaining biomass and facilitates disassembly of cellular bundles.

To further explore structural changes in the cellulose-enriched fractions, the Acetone-CF CEF samples were analyzed by TEM (Figure 10). This analysis revealed that the

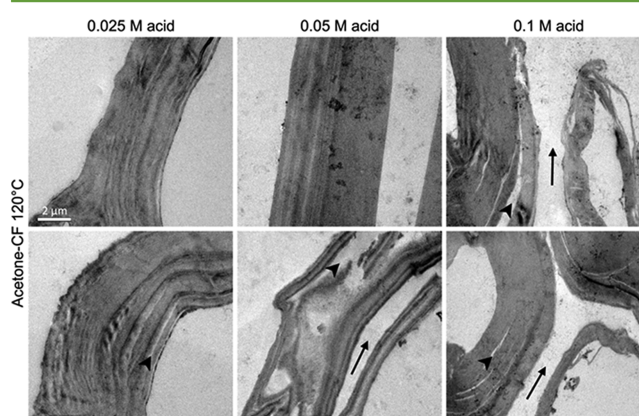


**Figure 10.** Transmission electron microscopy (TEM) of CF-CEF materials from treatment at 120 °C in Acetone-CF with various acid loadings. In addition to the disjoining of cells (arrows) observed by SEM, TEM analysis also revealed delamination within the cell walls (arrowheads) that was more extensive at the higher acid loadings.

mechanisms, including lignin removal, that caused the extensive separation of the corn stover tissue into individual cells extended into the layers of the cell walls. The CEF cell walls displayed delamination in the secondary walls that was more extensive with increasing acid concentration. This wall delamination combined with the cell separation creates large increases in surface area accessible to hydrolytic enzymes and increases diffusion pathways by which they may penetrate further into the cell walls.

**Solvent Recovery.** From the point of view of industrial scale-up, solvent recycling is an important factor. Therefore, MIBK recovery from Acetone-LEF and EtOH-LEF were conducted. MIBK recovered from Acetone-LEF and EtOH-LEF were 82.5% of and 103%, respectively.

## CONCLUSIONS

CF with a single-phase mixture of MIBK/EtOH/ $\text{H}_2\text{O}$  or MIBK/acetone/ $\text{H}_2\text{O}$  with catalytic amounts of sulfuric acid can readily separate the three major components (cellulose, hemicellulose, and lignin) in corn stover under mild conditions. For corn stover, Acetone-CF was found to be more efficient at fractionation given the omission of a salt-addition step to separate the organic and aqueous phases. Acid loading was found to have a greater impact on fractionation efficiency than

temperature for both CF pretreatments. For Acetone-CF, the glucan content in CEF was 88% and lignin content in LEF was 85% at 140 °C with 0.1 M acid, corresponding to 84% of the original glucan and 99% of the original lignin in corn stover. This indicates that the three main components in corn stover were well fractionated at the highest severity condition in Acetone-CF. The GPC analysis suggests that condensation reactions and cleavage of ether and/or ester linkages in corn stover lignin occurred with higher acid loadings. Electron microscopy of the tissue and cell wall morphology of the CEF samples revealed various degrees of cell separation and wall delamination that increased with treatment severity and extent of lignin extraction. These data indicate that the CF-CEF should be an excellent substrate for enzymatic hydrolysis to produce clean glucose because of higher glucan content and greater enzyme accessibility to the remaining cellulose, as will be reported in a future study. More generally, this study provides both detailed chemical insights into the resulting streams from CF pretreatment and mass balances required for conducting techno-economic analysis of organosolv fractionation.

## MATERIALS AND METHODS

**Materials.** Whole corn stover was knife-milled by a Wiley mill to pass through a 20-mesh screen. The composition of the corn stover was determined by the NREL standard method (Table 2).<sup>31</sup> Sucrose content in water extractives was measured by a YSI 2700 Select Biochemistry Analyzer. Sample moisture content was determined by a moisture analyzer (Mettler TOLEDO, HR83). The sulfuric acid, methyl isobutyl ketone (MIBK), and ethanol used were commercial grade.

**Clean Fractionation.** Whole corn stover (10 g) in a single-phase mixture of MIBK/EtOH/H<sub>2</sub>O or MIBK/acetone/H<sub>2</sub>O with sulfuric acid (0.025 to 0.1 M) was loaded into a 316 stainless steel pressure reactor. The reactor was sealed and heated in an electric heating block at 120 or 140 °C for 56 min. After the reaction, the reactor was cooled in ice water. The reaction mixture was separated into a solid fraction and an aqueous fraction via filtration. The solid fraction was thoroughly washed first with the same solvent (200 mL) followed by deionized H<sub>2</sub>O (650 mL). The solid fraction was air-dried at room temperature to obtain the cellulose-enriched fraction (CEF). Moisture content in CEF was measured by the moisture analyzer. The combined black filtrate (filtrate and wash liquors) obtained with EtOH-CF was mixed with solid NaCl (10 g/100 mL water contained in the solvent mixture) in a separatory funnel, shaken, and allowed to stand for 1 h to separate aqueous and organic phases. The aqueous layer was extracted with MIBK (48 mL) two times. MIBK layers were combined and washed with deionized H<sub>2</sub>O and brine, followed by evaporation in a rotavap to recover MIBK. The dried contents of the rotavap flask were further dried in a vacuum oven at 35 °C for 4 days to obtain the lignin-enriched fraction (LEF). The aqueous and organic phases present in combined black filtrate obtained with Acetone CF were separated with the addition of more MIBK (50 mL) without addition of NaCl. The aqueous layer was extracted with MIBK (28 mL) two times. The combined MIBK layers were treated similarly as described above for EtOH-CF. Compositional analyses of CEF and LEF were conducted according to the NREL method.<sup>31</sup> An aliquot of the aqueous layer was freeze-dried to obtain the dry hemicellulose-enriched fraction (HEF). The sugar and lignin contents in HEF were determined according to the NREL method. Briefly, to an aliquot of the aqueous layer, an equivalent weight of 72% H<sub>2</sub>SO<sub>4</sub> was added to obtain a 4 wt % H<sub>2</sub>SO<sub>4</sub> solution, which was then autoclaved at 121 °C for 1 h to hydrolyze the oligosaccharides into their monomers. Sugar recovery standards (SRS) were included to correct for degradation during autoclaving. The autoclaved samples were filtered, and the HPLC analysis of the filtrate provided carbohydrate analysis. The sugars and sugar degradation products were analyzed using a HPLC

equipped with refractive index and photodiode array detectors, respectively (Agilent 1100, Agilent Technologies, Palo Alto, CA). The monomeric sugars (glucose, xylose, and arabinose) in the filtrates were separated using a BIORAD Aminex HPX87H 300 mm × 7.8 mm ion exclusion column (catalogue no. 125-0140) maintained at 55 °C. The mobile phase (0.01 N sulfuric acid) was flowed at a rate of 0.6 mL/min. The sample injection volume was 20 μL, and the run time 45 min. The yield of each fraction was determined gravimetrically based on oven-dried whole corn stover.

The quantification of the MIBK solvent recovery was conducted from the LEF. After phase separation, the organic fraction was evaporated at 38 °C to collect all organic solvent that contains MIBK, mainly acetone, and a trace amount of water. The wt % of MIBK in the recovered solvent mixture was determined by GC-FID, and then the yield of recovered MIBK was calculated.

**GC-FID Analysis.** GC analysis was performed on an Agilent/HP 6890 GC-FID (Agilent Technologies, Palo Alto, CA). The MIBK mixture was separated using a 30 m × 0.32 mm × 0.25 μm Restek RTX-BAC1 column. Column conditions were as follows: A starting temperature of 35 °C was held for 3 min, ramped at 15 °C/min to 110 °C, and then continued at a ramped rate of 50 °C/min to 240 °C and held for 1 min. The carrier gas, He, was held at a constant flow of 3.0 mL/min.

**Gel Permeation Chromatography (GPC) Analysis.** LEF (20 mg) was acetylated in a mixture of pyridine (0.5 mL) and acetic anhydride (0.5 mL) at 40 °C for 24 h with stirring. The reaction was terminated by addition of methanol (0.2 mL) to neutralize the acetic anhydride. The acetylation solvents were then evaporated from the samples at 40 °C under a stream of nitrogen gas. The samples were further dried in a vacuum oven at 40 °C overnight. A final drying was performed under vacuum (1 Torr) at room temperature for 1 h. The dried acetylated LEF was dissolved in tetrahydrofuran (THF, Baker HPLC grade). The dissolved samples were filtered (0.45 μm nylon membrane syringe filters) before GPC analysis. The acetylated samples appeared to be completely soluble in THF. GPC analysis was performed using an Agilent 1050 HPLC with 3 GPC columns (Polymer Laboratories, 300 mm × 7.5 mm) packed with polystyrene-divinyl benzene copolymer gel (10 μm beads) having nominal pore diameters of 10<sup>4</sup>, 10<sup>3</sup>, and 10<sup>2</sup> Å. The eluant was THF, and the flow rate 1.0 mL/min. An injection volume of 25 μL was used. The GPC was attached to a diode array detector measuring absorbance at 260 nm (bandwidth 40 nm). Retention time was converted into molecular weight ( $M_w$ ) by applying a calibration curve established using polystyrene standards.

**Solid-State NMR.** High-resolution <sup>13</sup>C CP/MAS NMR measurements were carried out using a Bruker Avance 200 MHz spectrometer operating at 50.13 MHz at room temperature. The spinning speed was 7000 Hz, variable contact pulse, using a 50% ramp on the proton channel of 2 ms, acquisition time 32.8 ms, and delay between pulses of 1 s.

**HSQC NMR.** Heteronuclear single quantum coherence (HSQC) NMR spectra were acquired for LEFs. Each LEF (200 mg) was dissolved in DMSO-*d*<sub>6</sub> (1 mL) and filtered into an NMR tube through a cotton filter. Some LEFs prepared under milder CF conditions were partially soluble in DMSO-*d*<sub>6</sub>, while those fractionated under higher severity CF conditions were fully soluble. The solubility of LEFs probably depends on amount and DP of remaining carbohydrates in the LEFs. Spectra were acquired at 40 °C on a Bruker Avance III 600 MHz spectrometer at 11.7 T using a TCI cryoprobe. Spectra were acquired with 1024 points and a sweep width of 15 ppm in the F2 (<sup>1</sup>H) dimension and 512 points and SW = 220 ppm in the F1 (<sup>13</sup>C) dimension. For the lignin subunit analysis, integrations were performed on the peak representative of the  $\alpha$ -H correlation for  $\beta$ -O-4, oxidized  $\beta$ -O-4, phenylcoumarans, and dibenzodioxocin subunits. Original designations and assignments for these groups are given in Hoon 2008.<sup>32,33</sup>

**Fourier Transform Infrared (FTIR).** The FTIR spectrum of each LEF sample was obtained on a Nicolet 6700 FTIR spectrometer using a KBr beamsplitter. A deuterated triglycine sulfate (DTGS) detector was used to detect the IR signal and a Nicolet Smart iTR diamond

anvil attenuated total reflectance (ATR) cell was used for sample handling. The LEF sample was placed on the anvil and pressed into place with the iTR press. The sample was scanned 16 times at a mirror speed of 0.6329 cm/sec at a resolution of 4 cm<sup>-1</sup>. The single beam spectra were added and compared to a baseline spectrum of the diamond cell that had been acquired using the same parameters. The resulting spectra were corrected using a Mertz phase correction and a Norton–Beer apodization.

**Scanning Electron Microscopy (SEM).** SEM of CEF samples were performed using a FEI Quanta 400 FEG instrument. Samples were freeze-dried prior to imaging and mounted on aluminum stubs using conductive carbon tape and sputter coated with 10 nm of gold. Imaging was performed using beam-accelerating voltages ranging from 20 to 30 keV.

**Transmission Electron Microscopy (TEM).** TEM of CEF samples was performed using a FEI Tecnai G2 200 kV LaB6 instrument equipped with a 4 mega-pixel Gatan UltraScan 1000 camera. Samples were prepared by microwave-assisted processing as described previously.<sup>34</sup>

**X-ray Diffraction Measurements.** The crystallinity index (CrI) of CEF samples was measured by X-ray diffraction (XRD) by using a Rigaku (Tokyo, Japan) Ultima IV diffractometer with Cu K $\alpha$  radiation having a wavelength  $\lambda(K\alpha 1) = 0.15406$  nm generated at 40 kV and 44 mA. The results are shown in Table S5 of the Supporting Information. The diffraction intensities of freeze-dried CEF samples placed on a quartz substrate were measured in the range of 8–42° 2 $\theta$  using a step size of 0.02° at a rate of 2°/min. The CrI was calculated according to the amorphous subtraction method described by Park and co-workers.<sup>35</sup> Briefly, a diffractogram of a prepared amorphous cellulose sample was subtracted from the diffractograms of the CEF samples, and then the ratio of the integrated area of each subtracted diffractogram to the area of the original diffractogram was calculated and multiplied by 100.

## ■ ASSOCIATED CONTENT

### 🔗 Supporting Information

Figures and tables referenced in the main text, expanded data sets for composition and mass balances, crystallinity changes as a function of CF severity, and FTIR spectra of LEFs. This material is available free of charge via the Internet at <http://pubs.acs.org>.

## ■ AUTHOR INFORMATION

### Corresponding Author

\*E-mail: [Gregg.Beckham@nrel.gov](mailto:Gregg.Beckham@nrel.gov).

### Author Contributions

R. Katahira and A. Mittal have contributed equally to this work.

### Notes

The authors declare no competing financial interest.

## ■ ACKNOWLEDGMENTS

We acknowledge funding from the National Advanced Biofuels Consortium, funded by the U.S. Department of Energy (DOE), Bioenergy Technologies Office (BETO), through Recovery Act Funds and the U.S. DOE BETO.

## ■ REFERENCES

- (1) Eggeman, T.; Elander, R. T. Process and economic analysis of pretreatment technologies. *Bioresour. Technol.* **2005**, *96*, 2019–2025.
- (2) Mosier, N.; Wyman, C.; Dale, B.; Elander, R.; Lee, Y. Y.; Holtzapple, M.; Ladisch, M. Features of promising technologies for pretreatment of lignocellulosic biomass. *Bioresour. Technol.* **2005**, *96*, 673–686.
- (3) Wyman, C. E.; Dale, B. E.; Elander, R. T.; Holtzapple, M.; Ladisch, M. R.; Lee, Y. Y. Coordinated development of leading

biomass pretreatment technologies. *Bioresour. Technol.* **2005**, *96*, 1959–1966.

- (4) Wyman, C. E.; Dale, B. E.; Elander, R. T.; Holtzapple, M.; Ladisch, M. R.; Lee, Y. Y. Comparative sugar recovery data from laboratory scale application of leading pretreatment technologies to corn stover. *Bioresour. Technol.* **2005**, *96*, 2026–2032.

- (5) Wyman, C. E.; Dale, B. E.; Elander, R. T.; Holtzapple, M.; Ladisch, M. R.; Lee, Y. Y.; Mitchinson, C.; Saddler, J. N. Comparative sugar recovery and fermentation data following pretreatment of poplar wood by leading technologies. *Biotechnol. Prog.* **2009**, *25*, 333–339.

- (6) Tao, L.; Aden, A.; Elander, R. T.; Pallapolu, V. R.; Lee, Y. Y.; Garlock, R. J.; Balan, V.; Dale, B. E.; Kim, Y.; Mosier, N. S.; et al. Process and technoeconomic analysis of leading pretreatment technologies for lignocellulosic ethanol production using switchgrass. *Bioresour. Technol.* **2011**, *102*, 11105–11114.

- (7) Chundawat, S. P. S.; Beckham, G. T.; Himmel, M. E.; Dale, B. E. Deconstruction of lignocellulosic biomass to fuels and chemicals. *Annu. Rev. Chem. Biomol. Eng.* **2011**, *2*, 6.1–6.25.

- (8) Davis, R.; Tao, L.; Tan, E.; Bidy, M. J.; Beckham, G. T.; Scarlata, C.; Jacobson, J.; Cafferty, K.; Ross, J.; Lukas, J.; et al. *Process Design and Economics for the Conversion of Lignocellulosic Biomass to Hydrocarbons: Dilute-Acid Prehydrolysis and Enzymatic Hydrolysis Deconstruction of Biomass to Sugars and Biological Conversion of Sugars to Hydrocarbons*; Technical Report NREL/TP-5100-6022; National Renewable Energy Laboratory: Golden, CO, 2013.

- (9) Aden, A.; Foust, T. Technoeconomic analysis of the dilute sulfuric acid and enzymatic hydrolysis process for the conversion of corn stover to ethanol. *Cellulose* **2009**, *16*, 535–545.

- (10) Vicari, K. J.; Tallam, S. S.; Shatova, T.; Joo, K. K.; Scarlata, C. J.; Humbird, D.; Wolfrum, E. J.; Beckham, G. T. Uncertainty in technoeconomic estimates of cellulosic ethanol production due to experimental measurement uncertainty. *Biotechnol. Biofuels* **2012**, *5* (23).

- (11) Bozell, J. J.; Black, S. K.; Myers, M.; Cahill, D.; Miller, W. P.; Park, S. Solvent fractionation of renewable woody feedstocks: Organosolv generation of biorefinery process streams for the production of biobased chemicals. *Biomass Bioenergy* **2011**, *35*, 4197–4208.

- (12) Bozell, J. J.; O'Lenick, C. J.; Warwick, S. Biomass fractionation for the biorefinery: Heteronuclear multiple quantum coherence-nuclear magnetic resonance investigation of lignin isolated from solvent fractionation of switchgrass. *J. Agric. Food Chem.* **2011**, *59*, 9232–9242.

- (13) Zhang, Y. H. P.; Ding, S. Y.; Mielenz, J. R.; Cui, J. B.; Elander, R. T.; Laser, M.; Himmel, M. E.; McMillan, J. R.; Lynd, L. R. Fractionating recalcitrant lignocellulose at modest reaction conditions. *Biotechnol. Bioeng.* **2007**, *97*, 214–223.

- (14) Pan, X.; Arato, C.; Gilkes, N.; Gregg, D.; Mabee, W.; Pye, K.; Xiao, Z.; Zhang, X.; Saddler, J. Biorefining of softwoods using ethanol organosolv pulping: Preliminary evaluation of process streams for manufacture of fuel-grade ethanol and co-products. *Biotechnol. Bioeng.* **2005**, *90*, 473–81.

- (15) Fort, D. A.; Remsing, R. C.; Swatloski, R. P.; Moyna, P.; Moyna, G.; Rogers, R. D. Can ionic liquids dissolve wood? Processing and analysis of lignocellulosic materials with 1-n-butyl-3-methylimidazolium chloride. *Green Chem.* **2007**, *9*, 63–69.

- (16) Sun, N.; Rahman, M.; Qin, Y.; Maxim, M. L.; Rodriguez, H.; Rogers, R. D. Complete dissolution and partial delignification of wood in the ionic liquid 1-ethyl-3-methylimidazolium acetate. *Green Chem.* **2009**, *11*, 646–655.

- (17) Li, C. L.; Knierim, B.; Manisseri, C.; Arora, R.; Scheller, H. V.; Auer, M.; Vogel, K. P.; Simmons, B. A.; Singh, S. Comparison of dilute acid and ionic liquid pretreatment of switchgrass: Biomass recalcitrance, delignification and enzymatic saccharification. *Bioresour. Technol.* **2010**, *101*, 4900–4906.

- (18) Socha, A. M.; Plummer, S. P.; Stavila, V.; Simmons, B. A.; Singh, S. Comparison of sugar content for ionic liquid pretreated Douglas-fir woodchips and forestry residues. *Biotechnol. Biofuels* **2013**, *6* (61).

(19) Cruz, A. G.; Scullin, C.; Mu, C.; Cheng, G.; Stavila, V.; Varanasi, P.; Xu, D. Y.; Mentel, J.; Chuang, Y. D.; Simmons, B. A. Impact of high biomass loading on ionic liquid pretreatment. *Biotechnol. Biofuels* **2013**, *6*, 52.

(20) Sun, N.; Liu, H. B.; Sathitsuksanoh, N.; Stavila, V.; Sawant, M.; Bonito, A.; Tran, K.; George, A.; Sale, K. L.; Singh, S. Production and extraction of sugars from switchgrass hydrolyzed in ionic liquids. *Biotechnol. Biofuels* **2013**, *6*, 39.

(21) Black, S. K.; Hames, B. R.; Myers, M. D. Method of Separating Lignocellulosic Material into Lignin, Cellulose and Dissolved Sugars. U.S. Patent 5,730,837, 1998.

(22) Chum, H. L.; Johnson, D. K.; Black, S. K. Organosolv pretreatment for enzymic hydrolysis of poplars. 2. Catalyst effects and the combined severity parameter. *Ind. Eng. Chem. Res.* **1990**, *29*, 156–162.

(23) Overend, R. P.; Chornet, E. Fractionation of lignocellulosics by steam-aqueous pretreatments. *Philos. Trans. R. Soc., A* **1987**, *321*, 523–536.

(24) Weingarten, R.; Cho, J.; Conner, W. C.; Huber, G. W. Kinetics of furfural production by dehydration of xylose in a biphasic reactor with microwave heating. *Green Chem.* **2010**, *12*, 1423–1429.

(25) Wayman, M.; Lora, J. H. Aspen auto-hydrolysis – Effects of 2-naphthol and other aromatic compounds. *Tappi* **1978**, *61*, 55–57.

(26) Lora, J. H.; Wayman, M. Delignification of hardwoods by auto-hydrolysis and extraction. *Tappi* **1978**, *61*, 47–50.

(27) Gallagher, D. K.; Hergert, H. L.; Cronlund, M.; Landucci, L. L. In *Mechanism of Delignification in an Autocatalyzed Solvolysis of Aspen*. Proceedings of the 5th International Symposium on Wood and Pulp Chemistry, 1989; pp 709–717.

(28) Cybulska, I.; Brudecki, G.; Rosentrater, K.; Julson, J. L.; Lei, H. Comparative study of organosolv lignin extracted from prairie cordgrass, switchgrass and corn stover. *Bioresour. Technol.* **2012**, *118*, 30–36.

(29) Cybulska, I.; Brudecki, G. P.; Hankerson, B. R.; Julson, J. L.; Lei, H. Catalyzed modified clean fractionation of switchgrass. *Bioresour. Technol.* **2013**, *127*, 92–99.

(30) Donohoe, B. S.; Vinzant, T. B.; Elander, R. T.; Pallapolu, V. R.; Lee, Y. Y.; Garlock, R. J.; Balan, V.; Dale, B. E.; Kim, Y.; Mosier, N. S.; et al. Surface and ultrastructural characterization of raw and pretreated switchgrass. *Bioresour. Technol.* **2011**, *102*, 11097–11104.

(31) Sluiter, A. D.; Hames, B. R.; Ruiz, R. O.; Scarlata, C. J.; Sluiter, J. B.; Templeton, D. W.; Crocker, D. P. *Determination of Structural Carbohydrates and Lignin in Biomass: NREL Laboratory Analytical Procedure*; Technical Report NREL/TP-510-42618; National Renewable Energy Laboratory: Golden, CO, 2006.

(32) Hoon, K.; Ralph, J.; Akiyama, T. Solution-state 2D NMR of ball-milled plant cell wall gels in DMSO-d<sub>6</sub>. *BioEnergy Res.* **2008**, *1*, 56–66.

(33) del Rio, J. C.; Rencoret, J.; Prinsen, P.; Martinez, A. T.; Ralph, J.; Gutierrez, A. Structural characterization of wheat straw lignin as revealed by analytical pyrolysis, 2D-NMR, and reductive cleavage methods. *J. Agric. Food Chem.* **2012**, *60*, 5922–5935.

(34) Donohoe, B. S.; Ciesielski, P. N.; Vinzant, T. B. Preservation and Preparation of Lignocellulosic Biomass Samples for Multi-Scale Microscopy Analysis. In *Biomass Conversion: Methods and Protocols*; Himmel, M. E., Ed.; Humana Press: New York, 2012; pp 31–47.

(35) Park, S.; Baker, J. O.; Himmel, M. E.; Parilla, P. A.; Johnson, D. K. Cellulose crystallinity index: Measurement techniques and their impact on interpreting cellulase performance. *Biotechnol. Biofuels* **2010**, *3* (10).

(36) Resch, M. G.; Donohoe, B. S.; Ciesielski, P. N.; Nill, J. E.; Magnusson, L.; Himmel, M. E.; Mittal, A.; Katahira, R.; Bidy, M. J.; Beckham, G. T. Clean fractionation pretreatment reduces enzyme loadings for biomass saccharification and reveals the mechanism of free and cellulosomal enzyme synergy. *ACS Sust. Chem. Eng.* **2014**, DOI: 10.1021/sc500210w.